

The Application of a Quadrupole Mass Spectrometer to a Study of Methane Oxidation in Shock Waves

Yoshiaki HIDAKA, Midori NAGAYAMA, and Masao SUGA

Department of Chemistry, Faculty of Science, Ehime University, Bunkyo-cho, Matsuyama 790

(Received November 4, 1977)

A part of the mass-spectrometer shock-tube apparatus was improved, and its working characteristics were examined. The oxidation of methane was studied with this apparatus over the temperature range of 1800—2500 K and the total pressure range of 360—560 Torr at O_2/CH_4 ratios of 1—3. The induction period was measured by monitoring the oxygen concentration, and the following equation was found to hold:

$$\tau = 4.54 \times 10^{-10} [CH_4]^{0.37} [O_2]^{-0.64} \exp(35600/RT) \text{ s}$$

in which the concentrations were expressed in mol per cubic centimeter.

We have previously tried to apply a quadrupole mass spectrometer to fast reactions in shock waves, and have reported the devices and characteristics of the ion source.¹⁾ This mass-spectrometer shock-tube apparatus has since been used for the study of the decomposition of N_2O and C_2H_4 .²⁾ However, this apparatus still has two problems. One was that the rise time of the signal on the oscillogram is suddenly prolonged by the contamination of the ion-repeller electrode. The other is the overlapping of an abnormal signal with the monitored signal of the reactant or product; this abnormal signal does not come from any of the reactants or products.²⁾

The methane oxidation in a shock wave has been studied in detail by many investigators.^{3–16)} There is a tendency for the measured apparent activation energies to depend on the total experimental pressures, as has been mentioned by Cooke *et al.*¹⁵⁾ Therefore, it can be seen that the apparent activation energies previously reported may be classified roughly into two groups: about 33 kcal mol⁻¹ (below 1 atm) and 50 kcal mol⁻¹ (above 2 atm). The studies under low-pressure conditions (below 1 atm) are few in number than those at high pressures. It also has not become sufficiently apparent whether or not the apparent activation energy

at low pressures is lower than that at high pressures.

In the present paper, we wish to report on the improvement of the apparatus and its working characteristics. Another purpose of this paper is to confirm the apparent activation energy in the oxidation of methane at relatively low pressures (below 560 Torr).

Experimental

Apparatus. The scheme of the shock tube which connects with the quadrupole mass spectrometer is given in Fig. 1. The details of the shock tube have already been described.^{1,2)} In the present experiment, barium titanate gauges of G_2 and G_3 were used instead of platinum resistance gauges. The barium titanate gauge G_3 was mounted flush with the inside surface of the end wall of the shock tube. A pinhole leak 20 μ m in diameter was at the center of a small disk 10 mm in diameter and 1 mm thick, which was mounted flush with the inside surface of the end plate of the shock tube.

In the previous experiments, the quadrupole mass spectrometer and the shock tube were placed at right angles to one another so that the beam of gas molecules emerging from the pinhole leak entered into the ion source at right angles with the quadrupole Rod (L-type).¹⁾ In the present experiment, though, the quadrupole mass spectrometer and shock tube

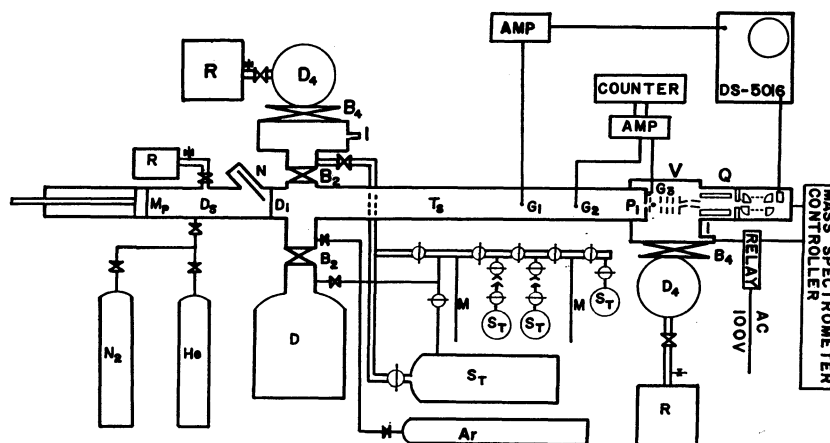


Fig. 1. Schematic diagram of the apparatus.

M_p : Movable piston, D_s : driver section, N : needle, D_i : diaphragm, D : dumping tank, B_2 : 2-inch butterfly valve, I : ionization gauge, B_4 : 4-inch butterfly valve, D_4 : 4-inch diffusion pump, R : rotary pump, S_T : storage tank, M : manometer, T_s : test section, G_1 , G_2 , G_3 : barium titanate pressure gauge, P_1 : pinhole leak of 20 μ m in diameter, V : vacuum chamber, Q : quadrupole mass spectrometer.

were placed at an angle of 180° to one another so that the beam of gas molecules might enter straightforwardly into the ion source from the opposite direction of the quadrupole Rod (I-type). A 4-inch oil diffusion pump with a liquid nitrogen trap was connected to the vacuum chamber, and the diffusion pump and the vacuum chamber were separated by a 4-inch butterfly valve.

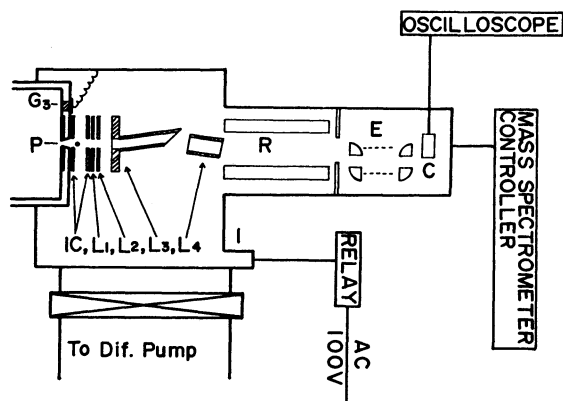


Fig. 2. Schematic diagram of the ion source, the vacuum chamber and the end section of the shock tube.

G_3 : Barium titanate pressure gauge, P: pinhole leak of $20\text{ }\mu\text{m}$, IC: ionization chamber, L_1 , L_2 , L_3 , and L_4 : ion lens electrodes, R: Rod, E: secondary electron multiplier, C: ion collector, I: ionization gauge.

A scheme of the ion source and the end section of the shock tube is shown in Fig. 2. The ion source consisted of the following parts: an ionization chamber (IC), an electron repeller (ER), a filament (F), an electron target (T), and focusing lenses (L_1 , L_2 , L_3 , and L_4). Most of the metal parts were made of stainless steel. The tungsten filament, which was 0.2 mm in diameter, was wound in a six-turn helix. The L_1 and L_2 lens electrodes were 4 mm in inner diameter and 0.5 mm long. The ion-lens electrodes of L_3 and L_4 were constructed of pipes 4 mm and 6 mm in inner diameter, and 40 mm and 30 mm in length, respectively. They were placed at an angle of 10° to the axis of the shock tube, and also the exit of the L_3 lens was cut at an angle of 30° , as is shown in Fig. 2. The electron inlet slit (1.5 mm in diameter) was devised so as to set the edge of the leak side of the ionization chamber as near as possible. Consequently, the distance between the pinhole and the electron-inlet slit was shortened to about 4 mm. The voltage supplied to each electrode of the ion source could be changed as follows:

$$V_{ER}: +30-150\text{ V}, \quad V_{IC}: +150-20\text{ V},$$

$$V_T: +150-30\text{ V}, \quad V_{L_1}, V_{L_2}, V_{L_3}: +150-110\text{ V},$$

$$V_{L_4}: +150-0\text{ V}.$$

Sample gases behind reflected shock waves were directly introduced into the ionization chamber through the pinhole leak $20\text{ }\mu\text{m}$ in diameter and were ionized in the ionization chamber. Then, the formed ions were extracted from the ionization chamber into the ion lenses and transported into the analyzer tube (the quadrupole Rod). The ions filtered by the Rod were led to the secondary electron multiplier, and the ion-current generated from the electron multiplier was measured by means of an oscilloscope (Iwatsu DS-5158).

Materials. The compositions of the reaction mixtures used were

(A) 1% CH_4 , 2% O_2 , 97% Ar,

(B) 1% CH_4 , 3% O_2 , 96% Ar,

(C) 2% CH_4 , 2% O_2 , 96% Ar.

The methane, oxygen, and argon were obtained from commercial cylinders; their purities were 99.9, 99.9, and 99.99% respectively. The initial pressures of the reaction mixtures were always about 10 Torr.

Procedure. The test section of the shock tube and the vacuum chamber in which the ion source had been installed were evacuated to 2×10^{-6} Torr and 3×10^{-7} Torr respectively by two pumping systems, both of which had 4-inch oil diffusion pumps with liquid nitrogen traps. When the sample gas of about 10 Torr was admitted into the test section of the shock tube, the pressure in the vacuum chamber normally indicated a value of 4×10^{-6} Torr. The driver section was evacuated by means of a rotary pump, prior to admitting the driver gas He, until the residual gas pressure was about 1×10^{-3} Torr. Shock waves were fired within two minutes after the isolation of the pumping system, because the leaking and outgassing rate of the test section was about 1.57×10^{-3} Torr l/min. The operations of the pinhole leak were always checked by monitoring the inside pressure of the vacuum chamber using the ionization gauge (I). That is, before each run, the pressure in the vacuum chamber must indicate the value of 4×10^{-4} Torr when dried nitrogen gas of about 1 atm is admitted into the test section; also, the pressure must indicate the value of 4×10^{-6} Torr when a sample gas of about 10 Torr is admitted into the test section.

On the other hand, the quadrupole mass spectrometer was always adjusted and checked thus:

(1) Each electrode voltage (V_{ER} , V_{IC} , V_T , V_{L_1} , V_{L_2} , V_{L_3} , and V_{L_4}) was tentatively set up so that the detecting sensitivity of the quadrupole mass spectrometer might become a maximum.

(2) Then, a standard gas whose composition was 2% N_2 + 98% Ar was heated by reflected shock waves, and the oscillogram of N_2 was observed by using the ion signal of the mass position, $m/e=28$. If necessary, the voltage, V_{L_3} , of the lens electrode (L_3) was readjusted so that the time-history curve of N_2 could level off to a constant value during about 1000 μs .

(3) This adjustment in (2) was made for each series of experimental runs. When the detecting sensitivity of the mass spectrometer became so low that the variation in the ion-current could not be observed, the ion source had to be cleaned. The adjustment as described above was then done again.

After a series of adjustments, the reaction mixtures were heated by reflected shock waves, and the oscillogram of O_2^+ ($m/e=32$) was monitored and analyzed. With a universal counter (Iwatsu US-6141) with a precision of $\pm 0.1\text{ }\mu\text{s}$, the velocity of the shock waves was determined by detecting their passage between two gauges, G_2 and G_3 . By assuming the gas to be ideal, the thermodynamic properties of the gas behind the reflected shock waves were calculated from the three conservation equations and from the measured incident-shock velocity.

Characteristics of Improved Ion Source. When we try to design an ion source for the study of fast reactions, the following requirements are essential, as was mentioned in a previous paper:¹⁾

(1) The molecules emerging from the pinhole at the end plate of the shock tube should be ionized fast.

(2) The ions thus formed should be extracted fast from

the ionization chamber.

(3) Unionized molecules should be withdrawn fast from the ionization chamber.

(4) Collisions of ions with neutral molecules emerging from the pinhole should be limited.

In the case of using the L type reported previously, ions formed by the electron bombardment needed to be forcibly extracted from the ionization chamber at right angles with the beam of the gas molecules emerging from the pinhole leak. An ion-repeller electrode had to be provided in the ion source so that the ion formed might be expelled effectively and quickly from the ionization chamber; consequently, at about 700 Torr (the pressure behind reflected shock wave) the rise time obtained was less than 10 μ s. When the ion-repeller electrode was omitted from this ion source, the rise time was above 150 μ s. The contamination on the ion-repeller electrode tended to increase in every experimental run and resulted in prolonging the rise time of an ion signal. This trouble happened irregularly and abruptly when the experimental runs were repeated more than 50 times. The complete adjustment of the rise time was not easy; indeed, it was the most difficult technique among the experimental procedures.

In the case of the I type, a fairly short rise time (20–50 μ s) could be obtained over the pressure range of 360–560 Torr in spite of omitting the ion-repeller electrode. Since the rise time is inversely proportional to the pressure of the reflected shock wave, it can be deduced that this value is close to that in the L type. We infer that the fairly short rise time was obtained in spite of omitting the ion-repeller electrode, because the molecules emerging from the pinhole leak enter the ionization chamber, and the ions formed by an electron bombardment are expelled from that chamber. The direction of these molecules and ions is the same as in the I type; moreover, these molecules flow with a large translation energy in the direction of the ion lenses.¹⁾

In the I type, the troubles in the rise time were eliminated. This may be because the ion-repeller electrode was omitted from the ionization source. The rise time did not vary even if the experimental runs were repeated more than 200 times.

There is another problem, "the abnormal signal." Since, in this kind of study, the reaction gas is generally diluted with large quantities of Ar, the high range of the detecting sensitivity of the multiplier and the amplifier needs to be employed for observing the time history of reactants or products on the oscillogram. When a high detecting sensitivity was used, an

abnormal signal was observed; it always had to be subtracted in the data analysis as if it were a background signal.²⁾ It was considered that this abnormal signal was not attributable to ions but to neutral species possessing a high translational energy.²⁾ In order to separate the ions and neutral species, the lenses of L_3 and L_4 were designed as is shown in Fig. 2. The abnormal signal could be almost eliminated by this device. By this improvement of the ion source, the sensitivity was lowered slightly, but both the resolution of the mass spectrometer and the rise time of the ion signal did not vary at all.

This apparatus had been previously checked with the time history of Ar^+ ($m/e=40$).²⁾ In the present experiment, it was checked with the time history of N_2^+ ($m/e=28$) using a gas mixture (2% N_2 +98% Ar). A typical time history of N_2^+ is shown in Fig. 3. In this checking, it is necessary that the time history of N_2^+ measured on the oscillogram rise rapidly and remain constant for more than 1000 μ s.

Results and Discussion

Some typical oscillograms of reactants (CH_4 and O_2) and the main products (H_2O , CO , and CO_2) near 1940 K are shown in Fig. 4. All of these are measured with a same ionizing energy of 24 eV. The time history of a product (H_2O , CO , or CO_2) keeps a base level for a certain time after shock heating, and then begins to rise gradually. On the contrary, the time history of a reactant (CH_4 or O_2) rises rapidly, keeps a nearly constant value for a while, and then falls exponentially until an equilibrium is reached. There is a lag time in the apparatus which has been defined as the time elapsing from the beginning of the reflected shock-wave signal to the beginning of the ion-current signal.¹⁾ If the induction period is calibrated by monitoring the time history of one of the products, the lag time needs to be measured in preliminary experiments beforehand.

In the present study, the induction period is defined as the time elapsing between the reflected shock arrival and the onset of the rapid decrease in the oxygen concentration; it is measured by monitoring the O_2^+ ($m/e=32$) signals at an ionizing energy of 110 eV, as is shown in Fig. 5. The induction period is calibrated as is shown in Fig. 6, which is obtained by averaging the noise of an observed signal (Fig. 5). Since "the lag time" of the apparatus is cancelled in the calibration in Fig. 6, it is not necessary to take account of this. This is a reason for monitoring the concentration of the O_2 reactant in a series of experimental runs.

In order to monitor the time history of O_2^+ , a high detecting sensitivity was required. A high ionizing energy 110 eV, was adopted in order to achieve a higher detecting sensitivity. When this high ionizing energy was adopted, many fragments appeared. When the ion signals at $m/e=16$ were monitored at the ionizing energy of 110 eV, it was the signal of CH_4^+ plus O^+ which was considered to consist of fragment ions of H_2O , CO , and CO_2 . When we monitored the concentration of CH_4 , the ionizing energy had to be kept lower at the expense of the detecting sensitivity. This was another reason to monitor the concentration of O_2 .

Table 1 summarizes the results of the induction periods, τ , together with the conditions of the experimental runs.

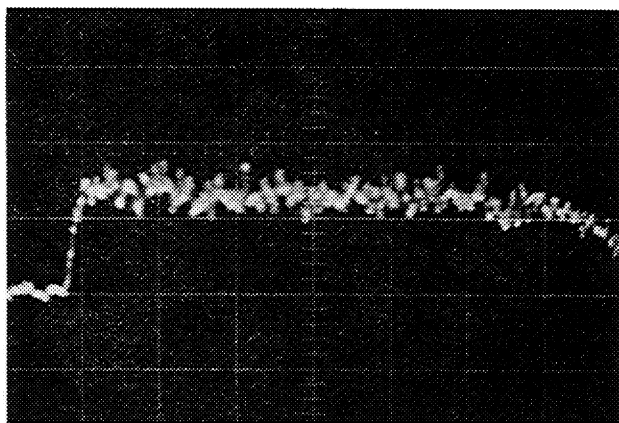


Fig. 3. Typical oscillogram of N_2^+ ($m/e=28$).

Sweep=200 μ s/div., $T_5=1908$ K, $P_5=430$ Torr. Supplied voltages: $V_{\text{ER}}=+22$ V, $V_{\text{IC}}=+130$ V, $V_{\text{T}}=+130$ V, $V_{\text{Li}}=+70$ V, $V_{\text{Ls}}=-116$ V, $V_{\text{Lr}}=+92$ V, $V_{\text{Ls}}=+110$ V, $V_{\text{Rod}}=+110$ V.

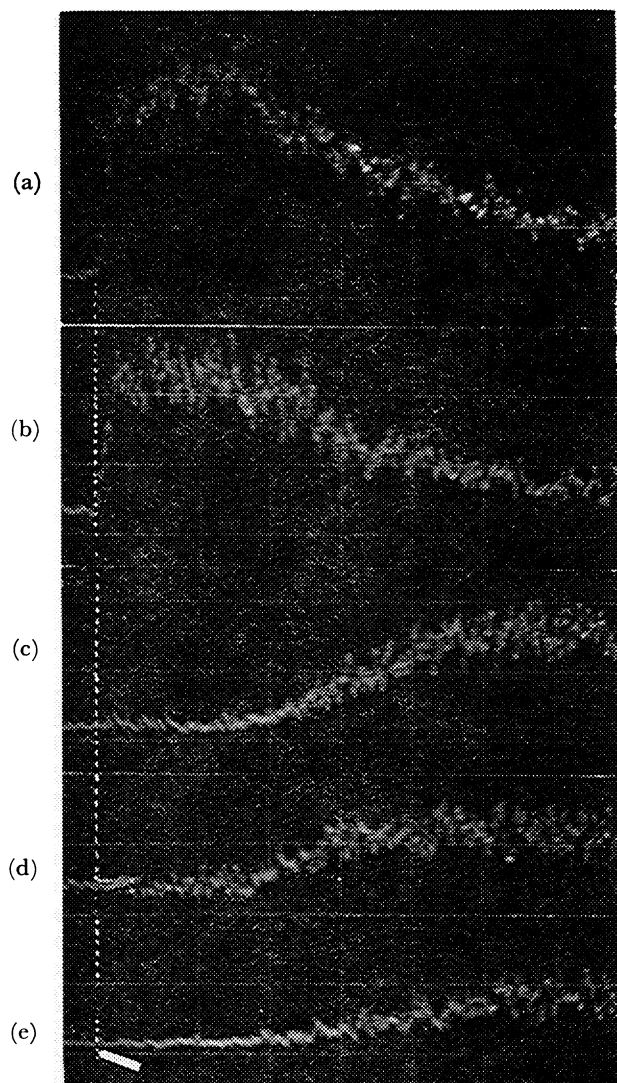


Fig. 4. Some typical oscillograms of species on the methane oxidation near 1940 K.

Sweep=200 μ s/div. (a) Time history curve of O_2^+ ($m/e=32$), $T_5=1956$ K, $P_5=416$ Torr. (b) Time history curve of CH_4^+ ($M/e=16$), $T_5=1944$ K, $P_5=413$ Torr. (c) Time history curve of H_2O^+ ($m/e=18$), $T_5=1936$ K, $P_5=412$ Torr. (d) Time history curve of CO^+ ($m/e=28$), $T_5=1938$ K, $P_5=412$ Torr. (e) Time history curve of CO_2^+ ($m/e=44$), $T_5=1947$ K, $P_5=414$ Torr. Supplied voltages: $V_{ER}=+18$ V, $V_{IC}=+44$ V, $V_T=+45$ V, $V_{L1}=+42$ V, $V_{L2}=-90$ V, $V_{L3}=+13$ V, $V_{L4}=0$ V, $V_{Rod}=+23$ V.

Figure 7 shows the plot of $\log \tau$ versus $1/T$ for three composition groups, A, B, and C. It can readily be seen that the values of $\log \tau$ in each group fall on a single line and that all the lines are parallel. Figure 8 shows the plotting of $\log \tau [CH_4]^{-0.37} [O_2]^{0.64}$ versus $1/T$ for the three groups of A, B, and C. All the points fit a single straight line. The temperature coefficient of the induction periods can be obtained from the slope of the line drawn in Fig. 8. Over the temperature range covered by the present experiment, the induction periods can be represented as

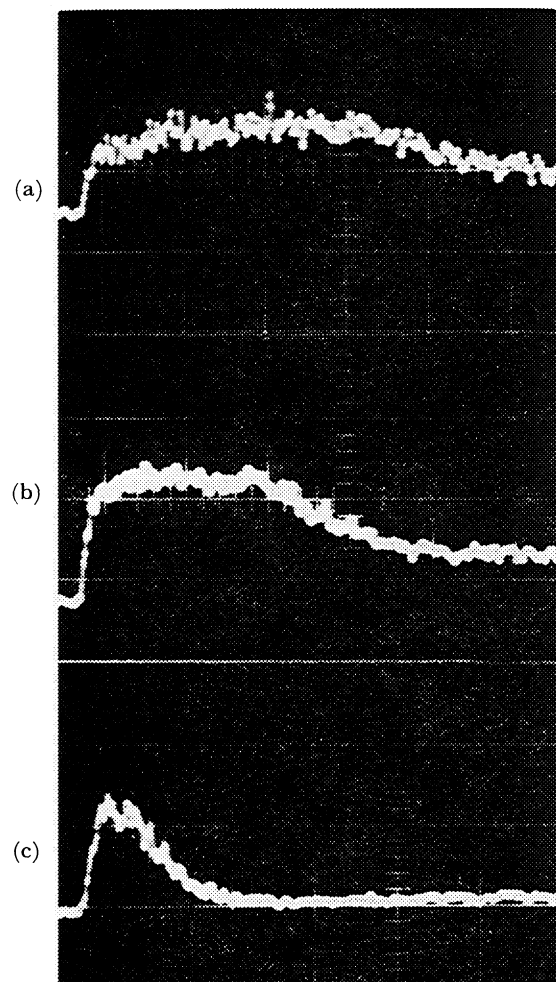


Fig. 5. Typical time history curves of O_2^+ ($m/e=32$), on oscillograms.

Sweep=200 μ s/div. Supplied voltages: $V_{ER}=+22$ V, $V_{IC}=+130$ V, $V_T=+130$ V, $V_{L1}=+70$ V, $V_{L2}=-116$ V, $V_{L3}=+92$ V, $V_{L4}=+110$ V, $V_{Rod}=+110$ V.

(a) Shock No. 110, (b) Shock No. 201, (c) Shock No. 310.

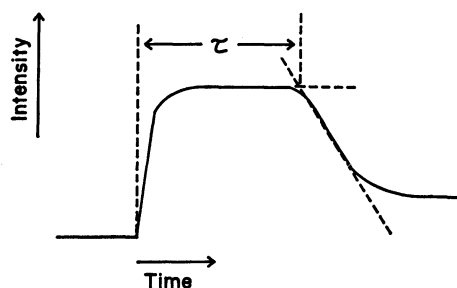


Fig. 6. Definition of the induction period.

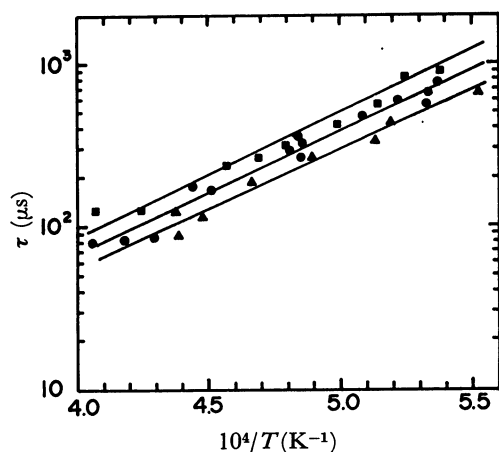
$$\tau = 4.54 \times 10^{-10} [CH_4]^{0.37} [O_2]^{-0.64} \exp(35600/RT) \text{ s,}$$

in which concentrations are expressed in mol per cubic centimeter.

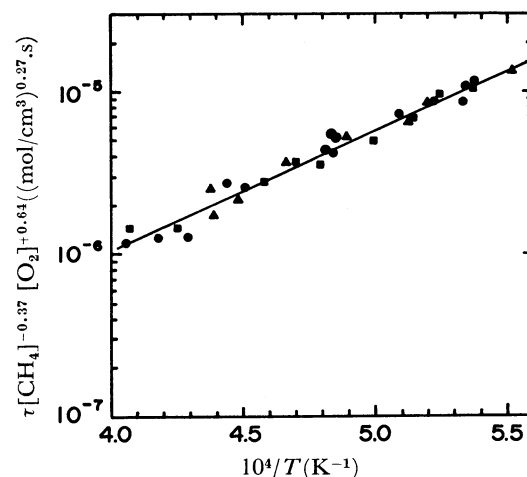
In the study of oxidation reactions in shock waves, induction periods have been considered to be a useful parameter in elucidating a reaction mechanism. The terms "induction period of ignition" and "induction period" have been used in studies of methane oxidation

TABLE 1. EXPERIMENTAL CONDITIONS
AND INDUCTION PERIODS

Series	Shock No.	T_5/K	P_5/Torr	$\tau/\mu\text{s}$
A	101	1860	389	741
	102	2060	447	339
	103	1875	393	551
	104	2390	553	81
	105	2220	499	167
	106	2328	535	82
	107	2068	453	345
	108	1965	437	470
	110	1877	394	680
	113	2080	457	281
	115	2253	511	172
	117	2465	578	79
B	119	2060	450	266
	120	1915	409	580
	201	1925	417	431
	203	2045	448	270
	204	2230	514	110
	207	2145	492	186
	208	2280	519	87
C	211	1813	487	648
	213	2285	524	125
	214	1950	425	330
	301	1907	406	815
	302	1945	417	560
	303	2087	462	300
	305	2355	549	125
	306	2130	576	255
	307	1862	392	890
	308	2005	435	415
	309	2187	494	235
	310	2458	579	125

Fig. 7. A plot of $\log \tau$ versus $1/T$ for three composition groups.

■: 2% CH_4 + 2% O_2 , ●: 1% CH_4 + 2% O_2 , ▲: 1% CH_4 + 3% O_2 .

Fig. 8. A plot of $\log \tau [\text{CH}_4]^{-0.37} [\text{O}_2]^{0.64}$ versus $1/T$ for three composition groups.

■: 2% CH_4 + 2% O_2 , ●: 1% CH_4 + 2% O_2 , ▲: 1% CH_4 + 3% O_2 .

using the shock waves although there is same uncertainty in their definitions. The first study of the induction period of methane oxidation in shock waves was carried out by Skinner and Ruehrwein in 1959.³⁾ Afterwards, a considerable number of data have been reported by many investigators.⁴⁻¹⁶⁾ Most of the reported activation energies center around 50 kcal/mol (at high pressures (above 2 atm)) or 33 kcal/mol (at low pressures (below 1 atm)).

Our experimental results indicate that the reaction of methane oxidation passes through two steps: the first step (during the induction period) is characterized by a very slow decrease in the oxygen concentration, while the second step (after the induction period) is followed by a rapid decrease. The induction periods are measured by monitoring the oxygen concentration; thereby, an apparent activation energy of 35.6 kcal/mol is obtained over the pressure range of 360–560 Torr and the temperature range of 1800–2500 K. The value of the apparent activation energy obtained is in good agreement with the values obtained by Cooke *et al.*,¹⁵⁾ Higgin *et al.*,¹⁰⁾ and Kistiakowsky *et al.*⁴⁾ in spite of the differences in the method of measurement. On the other hand, although we have tried analysing the time history of the O_2 concentration after the induction period, we have not yet obtained any useful information on the methane oxidation.

References

- 1) M. Suga and Y. Hidaka, *Mass Spectroscopy*, **23**, 23 (1975).
- 2) Y. Hidaka, *J. Sci. Hiroshima Univ., Ser. A*, **38**, 301 (1974).
- 3) G. B. Skinner and R. A. Ruehrwein, *J. Phys. Chem.*, **63**, 1736 (1959).
- 4) G. B. Kistiakowsky and L. W. Richards, *J. Chem. Phys.*, **36**, 1707 (1962).
- 5) H. Miyama and T. Takeyama, *J. Chem. Phys.*, **40**, 2049 (1963).
- 6) T. Asaba, K. Yoneda, N. Kakihara, and T. Hikita, "Symp. Combust. 9th," Academic Press (1963), p. 193.
- 7) H. Miyama and T. Takeyama, *Bull. Chem. Soc. Jpn.*,

38, 37 (1965).

8) G. P. Glass, G. B. Kistiakowsky, J. V. Michael, and H. Niki, "Symp. Combust. 10th," Combustion Institute (1965), p. 513.

9) R. I. Soloukhin, "Symp. Combust. 11th," Combustion Institute (1967), p. 671.

10) R. M. R. Higgin and A. Williams, "Symp. Combust. 12th," Combustion Institute (1969), p. 579.

11) D. J. Seery and C. T. Bowman, *Combust. Flame*, **14**, 37 (1970).

12) D. F. Cooke and A. Williams, "Symp. Combust. 13th," Combustion Institute (1971), p. 757.

13) A. Lifshitz, K. Scheller, A. Burcat, and G. B. Skinner, *Combust. Flame*, **16**, 311 (1971).

14) T. Tsuboi and H. G. Wagner, "Symp. Combust. 15th," Combustion Institute (1974), p. 883.

15) D. F. Cooke and A. Williams, *Combust. Flame*, **24**, 245 (1975).

16) A. Grillo and M. W. Slack, *Combust. Flame*, **27**, 377 (1976).
